Available online at www.sciencedirect.com
SCIENCE DIRECT®
Journal of Chromatography A, 1065 (2005) 59–67
JOURNAL OF CHROMATOGRAPHY A
www.elsevier.com/locate/chroma

# Pressure drop in CIM disk monolithic columns

Igor Mihelič[a], Damjan Nemec[b], Aleš Podgornik[c,*], Tine Koloini[d]

[a] *Melamin–Chemical Company, Tomšičeva 9, SI-1330 Kočevje, Slovenia*
[b] *National Institute of Chemistry, Hajdrihova 19, SI-1001 Ljubljana, Slovenia*
[c] *BIA Separations d.o.o., Teslova 30, SI-1000 Ljubljana, Slovenia*
[d] *Faculty of Chemistry and Chemical Technology, University of Ljubljana, Aškerčeva 5, SI-1000 Ljubljana, Slovenia*

Available online 19 November 2004

**Abstract**

Pressure drop analysis in commercial CIM disk monolithic columns is presented. Experimental measurements of pressure drop are compared to hydrodynamic models usually employed for prediction of pressure drop in packed beds, e.g. free surface model and capillary model applying hydraulic radius concept. However, the comparison between pressure drop in monolith and adequate packed bed give unexpected results. Pressure drop in a CIM disk monolithic column is approximately 50% lower than in an adequate packed bed of spheres having the same hydraulic radius as CIM disk monolith; meaning they both have the same porosity and the same specific surface area. This phenomenon seems to be a consequence of the monolithic porous structure which is quite different in terms of the pore size distribution and parallel pore nonuniformity compared to the one in conventional packed beds. The number of self-similar levels for the CIM monoliths was estimated to be between 1.03 and 2.75.


*Keywords:* Monoliths; Pressure drop; Hydraulic radius; Pore self-similarity; Parallel connectivity

## 1. Introduction

Chromatographic separations represent an important end-of-pipe process in the production of pharmaceutical and other life science goods due to the rather low reaction conversions and required high product purity. Because of that, purification is usually slow and very cost intensive. Considerable saving in capital investment as well as operational costs can be made by introducing new stationary phases and by understanding the fundamental phenomena taking place during these processes.

Classical particulate stationary phases for chromatographic separations are prepared by packing micrometer sized porous particles into a column. Separation of products takes place in the pores of particles and therefore the rate of separation is diffusion limited, meaning that the rate can be increased only on the expense of lower separation quality. In addition, the relatively low porosity of such columns gives rise to large pressure drops. Thus, monolithic stationary phases are becoming more and more important in the field of liquid chromatography because they enable extremely fast separations without changing the resolution and binding capacity [1,2]. Monoliths consist of single piece of highly porous organic or inorganic material with pores made up of highly interconnected channel network resulting in high effective porosity and thus enabling efficient flow of the mobile phase. As a result, fast mass transfer between the stationary and mobile phase is possible and, in addition, the pressure drop is considerably lower than with classic particulate stationary phases.

Several results have been published in the literature dealing with the pressure drop in monolithic columns. The main difficulty is how to properly describe their structural properties to be able to compare them with the particulate supports. The prerequisite for such a comparison is an introduction of a universal characteristic dimension for the description of the monolith structure. Several approaches have been proposed in the literature.

Meyers and Liapis used a pore-network modeling approach wherein a number of so-called flow nodes are inter-

* Corresponding author. Tel.: +386 1 426 56 49; fax: +386 1 426 56 50.
*E-mail address:* ales.podgornik@monoliths.com (A. Podgornik).

0021-9673/$ – see front matter © 2004 Elsevier B.V. All rights reserved.
doi:10.1016/j.chroma.2004.10.054

connected by cylindrically shaped pores with variable diameter [3–5]. To predict the pressure drop, detailed knowledge of the structural properties is required, such as pore size distribution and pore connectivity. The latter, however, is very difficult to determine, therefore the lack of accurate experimental data limits wider application of the model.

Tallarek and coworkers introduced equivalent particle dimension for silica monoliths [6,7]. This dimension is obtained by dimensionless scaling of macroscopic fluid behavior, i.e. hydrodynamic permeability and hydrodynamic dispersion in both types of material; particulate and monolithic. As a result there is no need for direct geometrical translation of their constituent unit. This elegant approach can be basically applied to any type of stationary phase. However, since there is no clear correlation to the monolith structural properties it is difficult to perform an optimization of the monolithic structure on its basis.

An even more detailed elaboration of the pressure drop prediction on silica monoliths was performed by Vervoort et al. [8,9]. Their calculations were based on computational fluid dynamics simulations using Navier–Stokes equations. The assumption of the tetrahedral skeleton structure enabled to correlate the pressure drop to the skeleton thickness and column porosity. Using this approach it is possible, on a theoretical basis, to predict optimal structure for the monolith and can therefore be used as a powerful optimization tool. However, so far this approach was only applied to the tetrahedral skeleton structure and its application on other types of monoliths having different structure might not be trivial. This is probably the reason why no attempts to describe methacrylate monoliths in a similar manner have been published.

Because the structure of methacrylate monoliths more resembles the particle beds attempts have been made to characterize them with the well-known Kozeny–Carman equation and calculation of the equivalent particle diameter from the pressure drop data have been made [10]. It was noticed that the calculated equivalent particle diameter significantly exceeded the size of the particles determined from SEM pictures. However, in more recent work published by the same group the discrepancy was found to be much smaller [11].

The aim of this work is an introduction of a different approach, based on the hydraulic radius calculation that could be applied on various types of chromatographic porous media enabling their comparison.

## 2. Experimental

### 2.1. Modeling

The most common approach for pressure drop modeling in packed beds is through the use of the so called *capillary model* where porous material is regarded as a bundle of tangled tubes of weird cross section. The theory can then be developed by applying the results of flow through a single straight tube to the collection of crooked tubes by using a hydraulic radius of the porous medium as a characteristic dimension of the hypothetical channels to which the porous medium is assumed to be equivalent. The hydraulic radius is defined as [12]:

$$r_h = \frac{\text{cross section available for flow}}{\text{wetted perimeter}} = \frac{\text{volume available for flow}}{\text{total wetted surface}} = \frac{\varepsilon}{a} \quad (1)$$

Since the channels need not be regular, the measure of the hydraulic radius in terms of the ratio of volume to the surface of the pore space, rather than the diameter of a hypothetical pore, can be used. As the flow rates through chromatographic columns are very low (in order to insure sufficient time for product separation and also to avoid excessive pressure drop) one can employ the Hagen–Poiseulle equation for laminar flow through pipes by introducing four times the hydraulic radius instead of the diameter of the pipe [13], thus

$$\Delta P = k_1 \frac{2\eta u L}{r_h^2} \quad (2)$$

where $k_1$ represents the correction factor for the hydraulic radius assumption, which for laminar flow gives too low a prediction of pressure drop for a given fluid flow rate. In addition, the correction factor also takes into account the non-idealities of the porous media as the tortuousity of pores, their connectivity and difference in their shape and sizes. In essence, the correction factor, $k_1$, should be determined experimentally for every porous media separately [13]. Eq. (2) is sufficient to describe the pressure drop in the monolith, however, in order to compare the results with an adequate packed bed the expression can be developed further. By introducing the hydraulic radius for a packed bed made up of particles of equal size and shape

$$r_h = \frac{\varepsilon V_p}{(1-\varepsilon) S_p} = \frac{d_p \varepsilon}{6(1-\varepsilon)} \quad (3)$$

and the superficial, rather than interstitial, velocity ($v = u/\varepsilon$) we obtain the well-known Kozeny–Carman relationship for creeping flow in packed beds

$$\Delta P = 72 k_1 \frac{\eta v L}{d_p^2} \frac{(1-\varepsilon)^2}{\varepsilon^3} \quad (4)$$

The factor $k_1$ is usually assumed constant (2.08 when the KC constant is 150 and 2.5 when the KC constant is 180) for the narrow range of porosities typically encountered in packed beds ($\varepsilon = 0.35$–$0.50$).

However, in order to compare the packed bed with a monolith at porosities typical for a monolith ($\varepsilon > 0.6$) a more detailed evaluation of $k_1$ is needed. This can be done by employing the *free surface model* (also referred to as the *drag model*) of Happel [14], which has been shown to be applicable to a wide range of porosities, also those well above 0.6, where the capillary model fails as the predicted pressure drop values are

too low. Two concentric spheres serve as a cell model for a random assemblage of spheres in a fluid flow field. Each cell contains a particle surrounded by a fluid envelope (the outside surface of which is assumed to be frictionless) and contains the same amount of fluid as the relative volume of fluid to particle volume in the entire assemblage. By employing the Navier–Stokes equations to describe the creeping fluid motion, Happel obtained the following expression:

$$\Delta P = 18\frac{\eta v L}{d_p^2}(1-\varepsilon) \times \left(\frac{3+2(1-\varepsilon)^{5/3}}{3-9/2(1-\varepsilon)^{1/3}+9/2(1-\varepsilon)^{5/3}-3(1-\varepsilon)^2}\right) \quad (5)$$

It is possible to express Eq. (5) in the form of Eq. (4) when the correction factor $k_1$ is defined as

$$k_1 = \frac{4\varepsilon^3}{(1-\varepsilon)} \times \left(\frac{3+2(1-\varepsilon)^{5/3}}{3-9/2(1-\varepsilon)^{1/3}+9/2(1-\varepsilon)^{5/3}-3(1-\varepsilon)^2}\right) \quad (6)$$

The correction factor $k_1$, as defined in Eq. (6), is a function of porosity only. The influence of porosity on correction factor ($k_1$) for a wide range of porosity is presented in Table 1. As can be seen, $k_1$ is more or less constant (to within 5%) for the range of porosities typically encountered in packed beds. On the other hand, the value of the correction factor starts increasing rapidly as the porosity of the medium increases above 0.6 and becomes undetermined as the porosity approaches 1. By using Eq. (6) for the correction factor calculation it is possible to predict a pressure drop in packed bed of uniformly sized spheres in large range of porosity. However, for other types of porous media, like monoliths, the correction factor has to be determined separately and can then be used as a comparison criterion between the two types of supports.

Table 1
The correction factor $k_1$ calculated from Eq. (6) according to the free surface model of Happel [14] for assemblage of uniformly sized spherical particles for different porosities

| $\varepsilon$ | $k_1$ |
|---|---|
| 0.3 | 2.22 |
| 0.4 | 2.27 |
| 0.5 | 2.37 |
| 0.6 | 2.55 |
| 0.7 | 2.90 |
| 0.8 | 3.61 |
| 0.9 | 5.67 |
| 0.99 | 35.8 |

### 2.2. Measurements

Commercial CIM DEAE disk monolithic columns from BIA Separations (Ljubljana, Slovenia) were employed as test material for measuring pressure drop. SEM picture of this material is presented in Fig. 1. These 3-mm thick and 12-mm diameter discs are usually employed for analytical purposes. Nevertheless, they are produced in the same manner as in-

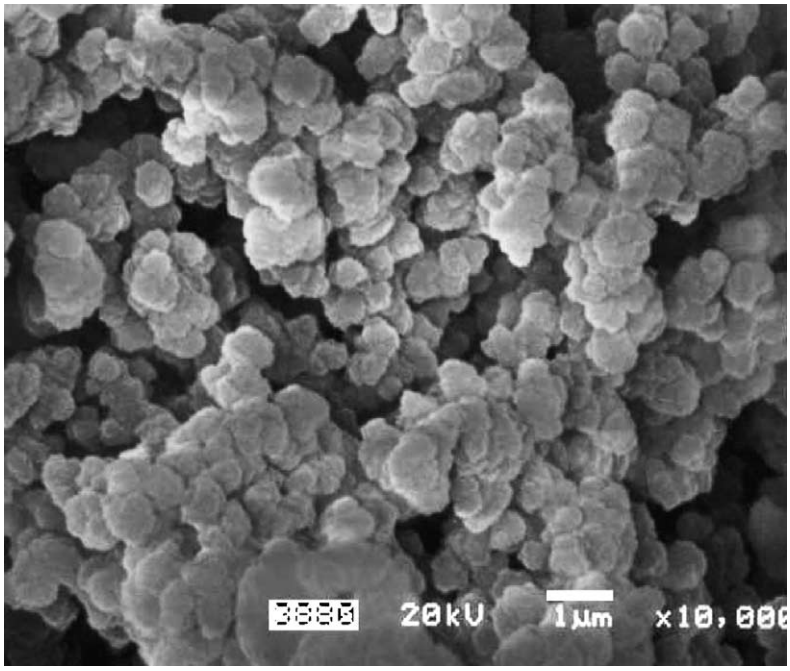


Fig. 1. SEM picture representing the structure of the GMA-EDMA monolith.

dustrial separation columns and thus have similar structural properties. The porosity and density of monolithic material were determined to be 0.64 and 0.48 mg/mL, respectively, using mercury porosimetry Pascal 440 (ThermoQuest Italia, Rodano, Italy). The specific surface area, determined by the BET method using Tristar 3000 (Micromeretics, Gosford, Australia) was found to be 7.19 $m^2$/g.

Pressure drop measurements were conducted by placing disks into stainless steel housing of the same dimensions as the commercially available ones. The experimental setup consisted of a Knauer 64 HPLC pump (Knauer, Berlin, Germany), digital pressure gauge Digibar from HBM (Darmstadt, Germany), the column and a digital GJC Instruments 5025000 flow meter (Merseyside, UK). These elements were connected with Peek standard tubing. The fluid employed in the experiments was bidestilated water at 20 °C. The pressure was measured directly at the column inlet, so no tubing was placed between the measurement point and the housing inlet. The column outlet was open to the atmospheric pressure; therefore the pressure drop on the column is equal to the measured value on the gauge.

## 3. Results and discussion

To estimate $k_1$ value for the methacrylate monoliths the pressure drop was measured. Data are shown in Fig. 2. The pressure drop is presented as a function of the flow rate and the length of monolithic layer. The column length was varied simply by adding 3 mm thick monolithic disks into the stainless steel housing. Monolithic disks cannot be used without the housing; therefore all presented results in Fig. 2 also include the pressure drop contribution of the housing. In the housing the distributor and collector represent the major contribution to pressure drop; however this contribution is still one order of magnitude lower than the pressure drop on a single monolithic column. Since the same housing was used for all experiments the pressure drop on the housing is not a

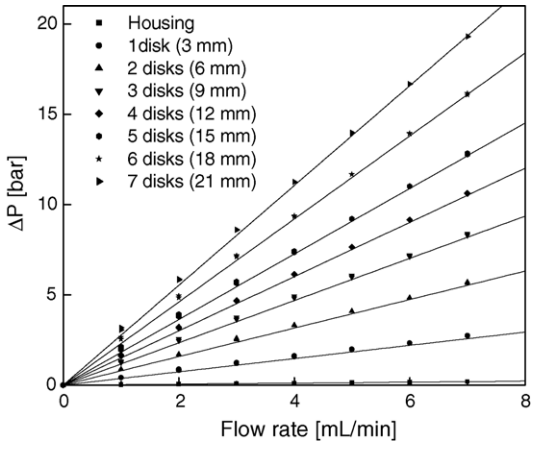


Fig. 2. The dependence of the measured pressure drop on the flow rate and the number of inserted monolithic disks, e.g. length of the monolithic layer.

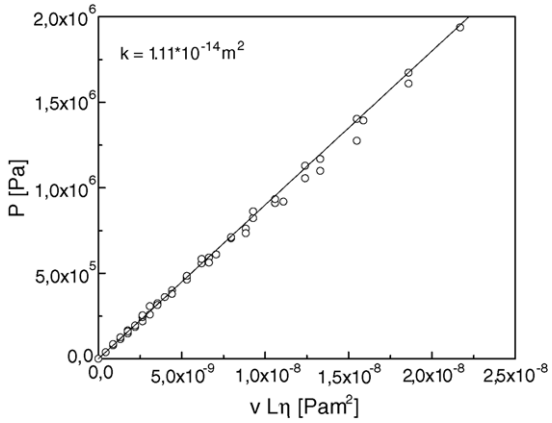


Fig. 3. The comparison between the experimentally measured data and Darcy's law. The permeability of the monolithic media is $1.11 \times 10^{-14}$ $m^2$.

function of the number of inserted disks and it can be subtracted as an end effect. Using this procedure, the dependence of the pressure drop on the length of monolithic layer can be calculated. It can be seen from Fig. 2 that the pressure drop is a linear function of flow rate, indicating a laminar flow regime. A linear relation between the pressure drop and the flow rate also proves that the porous monolithic structure is stable and does not contract at higher flow rates.

From the pressure drop data the permeability of the monolithic media can also be calculated. Accordingly to the Darcy's law, the dependence of pressure drop versus $vL\eta$ should be a linear function with the slope of inverse number of permeability. Such plot is presented in Fig. 3.

As expected, a straight line is found with the permeability of $1.11 \times 10^{-14}$ $m^2$ indicating that the Darcy law holds. Therefore, the assumption of laminar flow through the monolith has been justified experimentally.

Another parameter describing the characteristics of the porous monolithic material is the equivalent diameter. The equivalent diameter is defined as the diameter of the cylindrical channel in which the pressure drop would be equal to the pressure drop in the porous medium at the same interstitial velocity. It can be calculated according the Eq. (7):

$$D_E = \sqrt[2]{\frac{32\eta L \Phi_v}{\Delta P S \varepsilon}} \quad (7)$$

By using the measured data and applying Eq. (7) it is possible to calculate the equivalent diameter of the monolithic medium. Results of such a calculation are graphically presented in Fig. 4 as the dependence of equivalent diameter on the flow rate and the length of monolith.

It can be seen from Fig. 4 that the value of the equivalent diameter increases with the flow rate regardless of the monolithic layer length. There can be different reasons for such a behavior. The deviation is the most apparent at low flow rates which indicates the possibility of nonuniform distribution of the liquid over the column cross section. This reflects in the increased interstitial velocity that causes higher pressure drop

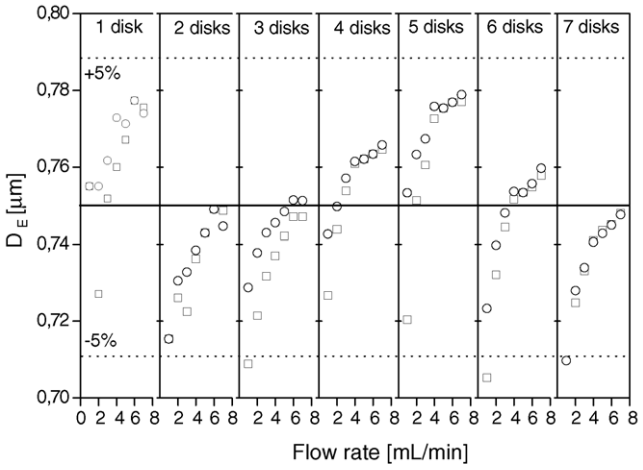


Fig. 4. The dependence of the calculated equivalent diameter on the flow rate and the length of the monolith. Symbols (□) and (◯) represent the two runs.

and accordingly to the Eq. (7) leads to lower equivalent diameter. At higher flow rates this effect slowly fades away and the equivalent diameter becomes more or less independent of the linear velocity. However, one would expect that this effect would diminish with the increase of the column length, since contribution of maldistribution would become smaller. Consequently, in the case of seven disks there should be significantly smaller differences by changing the flow rate as the measured 5% obtained for all measurements. An alternative explanation might be that some of the small pores, where the liquid is stagnant at low flow rates, become open at higher flow rates meaning appearance of a convective flow. Therefore, although being small, they do contribute to the overall value of the equivalent diameter. Similar hypothesis was put forth to explain longer retention volumes of oligonucleotides separated in isocratic mode on equal type of monolithic column [15].

Regardless of the true nature of the observed phenomenon, it can be concluded that the value of the equivalent diameter for the monolithic medium is 0.75 μm ±5%. The comparison between this value and the pore size distribution in CIM monoliths shows that the equivalent diameter is smaller than the diameter of macro pores having a median average diameter around 1.5 μm [16,17]. This means that the liquid must flow not only through macro pores but also through pores of smaller diameter, present in the structure.

For the determination of the hydraulic radius of the monolithic material a specific area available for flow and the effective porosity of the media must be known. Specific area of a typical chromatographic media is usually very high; however, the majority of the specific surface area is located within the closed pores that are not exposed to liquid flow. Therefore, the contribution of the closed pores area and void volume cannot be considered in Eq. (1). In methacrylate-based porous monolithic structure all pores are presumably open and available for flow, which can be seen from Fig. 1. Additional proof for the absence of closed pores in the monolithic structure is a very fast mass transfer in these media [11,18], because eventual presence of closed pores, where the liquid is stagnant, would results in much slower diffusion limited mass transfer. Consequently, it can be assumed that the entire measured specific area by BET method (7.19 $m^2/g$) corresponds to the area exposed to liquid flow. The specific surface area of the monolith can be also estimated from the scanning electron microscopy (SEM) pictures, presented in Fig. 1. It can be seen that the monolith consists of nonporous spherical particles with the diameter of approximately 0.6 μm that are glued together into clusters. Since these basic spherical constituents are not porous, the specific surface area can be calculated as in the case of loosely packed bed of spheres.

$$a = \frac{A}{m} = \frac{A}{\rho V} = \frac{6(1-\varepsilon)}{\rho d_p} = \frac{6(1-0.64)\times 10^{-6}\,m^3}{0.48\,g\ \ 0.6\times 10^{-6}\,m} = 7.5\,m^2/g \quad (8)$$

The difference between measured specific surface area by BET and calculated specific surface area is small, which proves that the spherical constituents are certainly nonporous. It can be concluded from this observation that the entire surface area of the monolith can be exposed to the liquid flow. Therefore the measured value of the specific surface area by BET can be applied in the Eq. (1) for the calculation of the hydraulic radius

$$r_h = \frac{\varepsilon}{\rho^a} = \frac{0.64\times 10^{-6}\,m^3\,g}{0.48\,g\times 7.19\,m^2} = 0.186\,\mu m \quad (9)$$

Using the known value of the hydraulic radius it is possible to fit measured pressure drop results (presented in Fig. 2) with Eq. (2) in order to determine the correction factor ($k_1$). In Fig. 5, the comparison between experimentally measured pressure drop and the prediction where $k_1 = 0.972$ is presented.

Such a low value of correction factor is very surprising. This means that the pressure drop in monolith is more than 50% lower than it would be in conventional packed bed, having the same porosity, hydraulic radius and length. Particle diameter having the same hydraulic radius as monolithic structure can be calculated from Eq. (3). Taking into account the same porosity (0.64) an adequate particle diameter is 0.63 μm. A packed bed of spheres with 0.63 μm in diameter, and bed porosity of 0.64 would have the same surface area as monolith. However, its pressure drop would be 2.75 times higher than in a monolith. This ratio can be easily determined from the comparison of correction factors. The correction factor for such a packed bed can be determined from Eq. (6) or by a quick interpolation of values given in Table 1 at 0.64 porosity, where $k_1 = 2.67$.

Furthermore, the fact that the correction factor $k_1$ for the monolith is lower than 1 is very unusual. This means that the

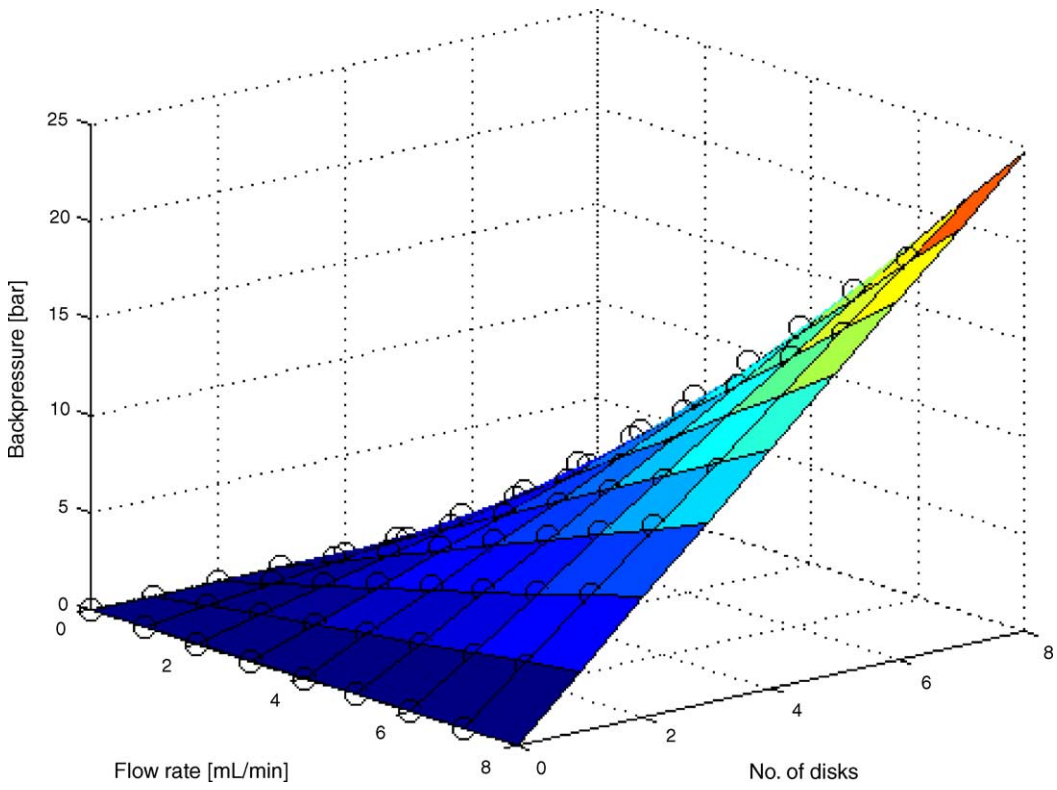


Fig. 5. Comparison between experimentally measured data and capillary model (Eq. (2)), where $k_1 = 0.972$.

pressure drop in a monolith is even lower that it would be in a bed made of equal and straight cylindrical tubes, having the same hydraulic radius as the monolithic column. Since this is not in accordance with standard models, at least one of the assumptions applied for derivation of Kozeny–Carman or Happel equations (for more details see Scheidegger [19]) may not be fulfilled in this case. The most obvious candidate is the assumption of uniform pores, whereas methacrylate monoliths are known to have bimodal pore distribution [16], which hardly fits the above assumption. This, however, is important since in heterogeneous porous structures with a parallel type of pore nonuniformity the majority of liquid flows through bigger channels while smaller channels remain permeable and therefore contribute to overall surface area [12]. Since bigger and smaller channels are highly interconnected they can be considered as randomly distributed. For such type of supports it was theoretically predicted that the throughput at a certain pressure drop increases significantly with the increase of the self-similarity levels when the porous structure is partially fractal [20]. This can also be demonstrated by simple calculation presented in Appendix [21]. On the basis of that calculation, the pressure drop in a structure of parallel type pore nonuniformity can be several times lower compared to the one with uniform pores, despite both having the same porosity. That the methacrylate based monoliths express certain degree of fractality and consequently, certain degree of self-similarity was already speculated by Podgornik [22] based on the SEM pictures of the structure (see Fig. 1) and the formation mechanism. The monolith skeleton is formed through the precipitation of nuclei into inert solvent. After precipitation they continue to grow and start to link together forming larger clusters and finally a rigid monolithic skeleton as described in details elsewhere [23]. Therefore, it is reasonable to assume that such structure possess certain degree of self-similarity resulting also in bimodal (or even multimodal) pore size distribution, as demonstrated by measurements performed with mercury porosimetry [16]. If we assume that the diameter ratio between larger and smaller pores is around or even above 10 (1500 nm is a diameter of large pores while the majority of the small pores has a diameter below 100 nm [16,17]), taking into account the obtained $k_1$ value, as well as the conclusions from Appendix, especially the one from Eq. (A.6), one can estimate that the methacrylate monoliths exhibit self-similarity level slightly above 1 (namely $1/0.972 = 1.03$). This conclusion would be valid in case the pores in the monolith would be straight cylindrical pores, for which the $k_1$ would be 1. We can see from the Fig. 1, however, that this is not the case and the structure more resembles a particulate bed. For such a structure, where tortuosity and other effects are taken into account, an equivalent $k_1$ would be 2.67. This value should be therefore compensated by a parallel pore structure and in this case the level of self-similarity would need to be (according to Eq. (A.7), Appendix) approximately 2.67/0.972 giving 2.75. The real value should therefore be between the two calculated values.

According to our best knowledge, this seems to be the first physical proof that heterogeneous and partially self-similar (fractal) porous structures are advantageous in terms of lower pressure drop over homogenous porous structures. Calculations performed in Appendix also demonstrate that it is extremely important to determine the type of pore connectivity in terms of the mobile phase flow to be able to properly predict and evaluate hydrodynamic properties of such units.

## 4. Conclusions

Unexpectedly low-pressure drop on monolithic column when compared with packed bed of spheres can be attributed to the monolith highly interconnected porous structure, bimodal pore size distribution and parallel type pore nonuniformity. Correction factor $k_1$ was shown to be for a methacrylate monolith only 0.972, while the correction factor for packed beds of spheres is 2.67 for the same porosity. The value below 1 indicates that it is possible to prepare monoliths having a pressure drop lower than in straight cylindrical pores if the proper architecture of the pores is present. Since the monolithic structure gives greater flexibility in terms of skeleton geometry in comparison to beads, we believe that by applying the proposed approach further optimization of monolithic porous structure is possible in order to achieve even lower pressure drops without significantly influencing chromatographic properties. The main goal would be to prepare the monoliths with even higher degree of self-similarity of a parallel type.

## Nomenclature

| | |
|---|---|
| $A$ | surface area ($m^2$) |
| $a$ | specific surface area ($m^2/g$) |
| $D_E$ | equivalent diameter (m) |
| $D_i$ | diameter of pore i (m) |
| $d_p$ | diameter of a sphere (m) |
| $k_1$ | correction factor |
| $L$ | length (m) |
| $m$ | mass (g) |
| $n$ | number of self-similar levels (/) |
| $N$ | pore diameter ratio (/) |
| $r_h$ | hydraulic radius (m) |
| $S$ | cross-sectional column area ($m^2$) |
| $S_p$ | particle surface ($m^2$) |
| $u$ | interstitial velocity (m/s) |
| $v$ | superficial velocity (m/s) |
| $V$ | volume ($m^3$) |
| $V_p$ | particle volume ($m^3$) |

*Greek symbols*

| | |
|---|---|
| $\Delta P$ | pressure drop (Pa) |
| $\Delta P_i$ | pressure drop on part i (Pa) |
| $\varepsilon$ | effective porosity (/) |
| $\Phi_v$ | volumetric flow rate ($m^3/s$) |
| $\eta$ | viscosity (Pas) |
| $\rho$ | density (kg/L) |

## Acknowledgement

We acknowledge to the Ministry of Education, Science and Sport of the Republic of Slovenia for support of this work through the grant P2-0191.

## Appendix A

Estimation of the pressure drop for different types of porous media.

In Fig. A.1, three types of pore arrangements are shown. In the first case (A), the structure is made of uniform pores all having equal diameter $D_a$. Structures B and C represent two extreme types of nonuniform pore distribution: B is a structure of parallel type pore nonuniformity and C is a serial type of pore nonuniformity. While the structure B is identical between all the nodes, the structure C is periodically changing. In reality, a combination of both types occurs and it is therefore difficult to predict the overall effect of the structure on the pressure drop. However, it is rather simple to calculate pressure drop for both extremes.

Let us assume that porosity is in all cases the same, meaning that the pore volume must be equal, as well that nodes have no volume, and therefore all the volume is in the pores. Furthermore, structures B and C have also the same hydraulic radius. For the beds of the same length, the pore area should be equal too. The same flow rate is applied to all structures.

It is clear that for structure A, having uniform pores, $\Delta P_{a1} = \Delta P_{a2}$ holds and consequently, the total pressure drop over the bed is $\Delta P_a = \Delta P_{a1} + \Delta P_{a2}$. For the structure B, pores $D_{b1}$ and $D_{b2}$ just switched their positions before and after the node, the pressure drop for both segments should be equal too, $\Delta P_{b1} = \Delta P_{b2}$ and overall pressure drop is $\Delta P_b = \Delta P_{b1} + \Delta P_{b2}$. Structure C is similar to structure B in terms of pore size distribution, since $D_{c1} = D_{b1}$ and $D_{c2} = D_{b2}$. However, since the pores in segment above the node have larger diameter of that below the node, $\Delta P_{c1} \neq \Delta P_{c2}$ while the total pressure drop is still $\Delta P_c = \Delta P_{c1} + \Delta P_{c2}$.

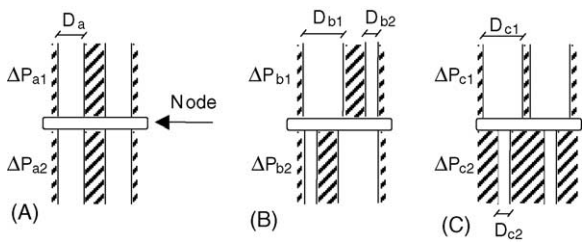


Fig. A.1. Different configurations of three hypothetical porous structures.

Liquid flowing through the pores can randomly switch through the nodes from one pore into another. Since in the case of methacrylate monoliths pores are highly interconnected, liquid should pass many nodes during its travel through the monolith, therefore the average passage time obeys Gauss distribution function according to the central limiting theorem [24].

Estimation of the pressure drop for structures A, B and C is performed in the following way. If we set that $D_{b1} = N \times D_{b2}$ ($N > 1$), the equality for the pore volume can be written as:

$$4\frac{\pi D_a^2}{4} = 2\frac{\pi D_{b1}^2}{4} + 2\frac{\pi D_{b2}^2}{4} = \frac{\pi D_{b1}^2}{2}\left(1 + \frac{1}{N^2}\right) = 2\frac{\pi D_{c1}^2}{4} + 2\frac{\pi D_{c2}^2}{4} = \frac{\pi D_{c1}^2}{2}\left(1 + \frac{1}{N^2}\right) \quad (A.1)$$

Flow through the bed should be equal to the sum of the flows through all the pores. Due to the cylindrical pore shape and laminar flow, pressure drop can be calculated according to the Hagen–Poiseulle equation (Eq. (2)) giving the following expression:

$$\Phi_v = 4\frac{\pi \Delta P_{a1} D_a^4}{128\eta L} = 2\frac{\pi \Delta P_{b1} D_{b1}^4}{128\eta L} + 2\frac{\pi \Delta P_{b1} D_{b1}^4}{N^4 128\eta L} = 2\frac{\pi \Delta P_{c1} D_{c1}^4}{128\eta L} + 2\frac{\pi \Delta P_{c2} D_{c2}^4}{128\eta L} \quad (A.2)$$

From the above equation it is easy to calculate the pressure ratio $\Delta P_a/\Delta P_b$

$$\frac{\Delta P_a}{\Delta P_b} = \frac{2(1 + 1/N^4)}{(1 + 1/N^2)^2} \quad (A.3)$$

Calculation of the $\Delta P_a/\Delta P_c$ ratio requires additional assumption that flow through the segment above the node is equal to the flow through the segment below the node and for structure C this gives

$$2\frac{\pi \Delta P_{c1} D_{c1}^4}{128\eta L} = 2\frac{\pi \Delta P_{c2} D_{c2}^4}{128\eta L} \quad (A.4)$$

$\Delta P_a/\Delta P_c$ ratio can then be rewritten as

$$\frac{\Delta P_a}{\Delta P_c} = \frac{8}{(1 + N^4)(1 + 1/N^2)^2} \quad (A.5)$$

Eqs. (A.3) and (A.5) are valid for two sizes of pores having the ratio of diameter $N$. In case there are many self-similar levels, it means levels of pores having the same diameter ratio, the Eqs. (A.3) and (A.5) can be generalized to

$$\frac{\Delta P_a}{\Delta P_b} = \frac{n\sum_{i=0}^{n-1} N^{-4i}}{\left(\sum_{i=0}^{n-1} N^{-2i}\right)^2} = n\frac{N^{-2} - 1}{N^{-2} + 1}\frac{N^{-2n} + 1}{N^{-2n} - 1} \quad (A.6)$$

with the limits

$$\lim_{N\to\infty} \frac{\Delta P_a}{\Delta P_b} = n \quad \text{and} \quad \lim_{n\to\infty} \frac{\Delta P_a}{\Delta P_b} = \infty \quad (A.7)$$

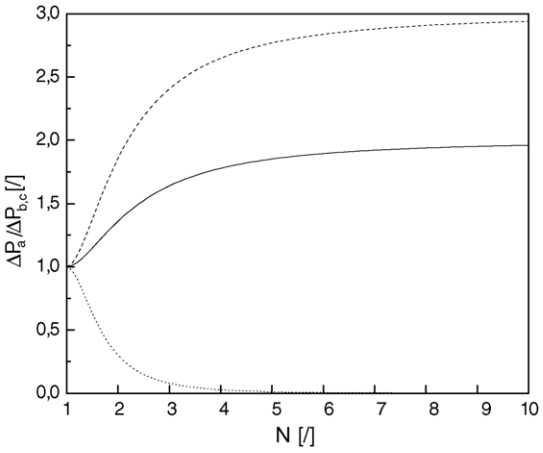


Fig. A.2. Dependence of $\Delta P_a/\Delta P_b$ and $\Delta P_a/\Delta P_c$ ratios on value of $N$. Solid line represents structure B having two pore sizes ($n = 2$), dashed line represents structure B having three pore sizes ($n = 3$) and dotted line represents structure C having two pore sizes ($n = 2$).

and

$$\frac{\Delta P_a}{\Delta P_c} = \frac{n^3}{\sum_{i=0}^{n-1} N^{4i}\left(\sum_{i=0}^{n-1} N^{-2i}\right)^2} = n^3\frac{N^4 - 1}{N^{4n} - 1}\left(\frac{N^{-2} - 1}{N^{-2n} - 1}\right)^2 \quad (A.8)$$

with the limits

$$\lim_{N\to\infty} \frac{\Delta P_a}{\Delta P_c} = 0 \quad \text{and} \quad \lim_{n\to\infty} \frac{\Delta P_a}{\Delta P_c} = 0 \quad (A.9)$$

where $n$ stands for number of self-similar levels (degree of self-similarity).

The effect of the structure type on the pressure drop it is demonstrated in Fig. A.2.

From the Fig. A.2, it is clear that structure B always gives lower value for the pressure drop in comparison to the uniform pore size distribution, while the structure C always gives higher pressure drop. In fact, both limits of $\Delta P_a/\Delta P_c$ when $n$ and $N$ goes to infinity go to 0 which means that $\Delta P_c$ goes to infinity. On the other hand, from the Eqs. (A.6) and (A.7) it is clear that when the pore ratio approaches infinity ($N\to\infty$) the ratio of the pressure drop $\Delta P_a/\Delta P_b$ equals to levels of self-similarity $n$ and consequently, when $n$ rises towards infinity the $\Delta P_b$ goes to zero. Theoretically speaking, with the proper pore size distribution and network architecture one can obtain as low pressure drop as desired for a given porosity. However, in practice there is a lower limit of the pore size through which the liquid flows, therefore further experiments are required to investigate what pressure drops can actually be achieved.

## References

[1] A. Štrancar, M. Barut, A. Podgornik, P. Koselj, Dj. Josić, A. Buchacher, LC GC 11 (1998) 660.
[2] G. Iberer, R. Hahn, A. Jungbauer, LC GC 17 (1999) 998.
[3] J.J. Meyers, A. Liapis, J. Chromatogr. A 827 (1998) 197.
[4] J.J. Meyers, A. Liapis, J. Chromatogr. A 852 (1999) 3.
[5] A. Liapis, J.J. Meyers, O.K. Crosser, J. Chromatogr. A 865 (1999) 13.
[6] U. Tallarek, F.C. Leinweber, A. Seidel-Morgenstern, Chem. Eng. Technol. 25 (2002) 1177.
[7] F.C. Leinweber, U. Tallarek, J. Chromatogr. A 1006 (2003) 207.
[8] N. Vervoort, P. Gzil, G. Baron, G. Desmet, Anal. Chem. 75 (2003) 843.
[9] N. Vervoort, P. Gzil, G. Baron, G. Desmet, J. Chromatogr. A 1030 (2004) 177.
[10] R. Hahn, A. Jungbauer, Anal. Chem. 72 (2000) 4858.
[11] A. Zöchling, R. Hahn, K. Ahrer, J. Urthaler, A. Jungbauer, J. Sep. Sci. 27 (2004) 819.
[12] F.A.L. Dullien, Porous Media: Fluid Transport and Pore Structure, second ed., Academic Press, Washington, DC, 1992.
[13] R.H. Perry, D.W. Green, Perry's Chemical Engineering Handbook, seventh ed., McGraw-Hill, New York, 1997.
[14] J. Happel, AIChE J. 4 (1958) 197.
[15] A. Podgornik, M. Barut, J. Jančar, A. Štrancar, J. Chromatogr. A 848 (1999) 51.
[16] M. Barut, A. Podgornik, M. Merhar, A. Štrancar, in: F. Švec, T.B. Tennikova, Z. Deyl (Eds.), Monolithic Materials: Preparation, Properties, and Applications, Elsevier, Amsterdam, 2003, p. 51.
[17] BIA Separations, http://www.biaseparations.com, 2004.
[18] I. Mihelič, T. Koloini, A. Podgornik, A. Štrancar, J. High Resolut. Chromatogr. 23 (2000) 39.
[19] A.E. Scheidegger, The Physics of Flow Through Porous Media, University of Toronto Press, Toronto, 1974.
[20] A.I. Liapis, Math. Modell. Sci. Comput. 1 (1993) 397.
[21] I. Mihelič, Ph.D. thesis, University of Ljubljana, Ljubljana, 2002.
[22] A. Podgornik, Ph.D. thesis, University of Ljubljana, Ljubljana, 1998.
[23] F. Švec, J.M.J. Frechet, Chem. Mater. 7 (1995) 707.
[24] E. Kreyszig, Advanced Engineering Mathematics, eighth ed., John Wiley & Sons, New York, 1999.